Analysis and Simulation of an Optimal Control Model of an Oyster Population Displaying an Allee Effect

Timothy R. McDade

Department of Mathematics,

College of William and Mary,

Williamsburg, VA 23187-8795, USA

Email: trmcdade@email.wm.edu

April 23, 2012

Abstract

During the last century, the oyster population of the Chesapeake Bay area has diminished greatly due to overfishing, pollution and climate change. Our Optimal Control model finds a sustainable solution that balances oyster harvesting with the health of the population. We wish to find the value of our Effort (control) function that harvests the most oysters possible without fishing the population to extinction. We create a Hamiltonian function and apply Bang-Bang Control in order to find a singular E^* between 0 and E_{max} such that E^* will balance out with the natural growth rate of the population to form a constant, stable population. Our model uses analytical and numerical solutions to determine the optimal sustainable population (N^*) and effort (E^*) for a Bang-Bang Control model. The analytical model also solves for times T_1 and T_2 at which the piecewise Heaviside effort function switches values of $E(t)$. In marine population study, there has not been extensive use of mathematics, especially optimal control theory. Consequently, as seen in our Future Work section, there is much room for expansion upon current scholarship regarding optimal control theory. Only by incorporating several environmental factors can one succeed in using mathematics to develop a successful harvesting strategy.

Contents

List of Figures

Chapter 1

Introduction

1.1 Background

During the last century, the oyster population of the Chesapeake Bay area has diminished greatly due to overfishing, pollution and climate change. Harvests since 1900 have decreased by two orders of magnitude, reaching their peak in 1884 at 615,000 tons [8, 11]. In 1992 the harvests were only 12,000 tons [8].

During the latter part of the 20th century, disease, extremes of salinity, and pollution took a toll on the oyster population throughout the Chesapeake Bay watershed. Increased flow of sediment into the Chesapeake Bay and its tributaries has raised sediment levels in the water, degrading the health of the oysters, lowering their fertility and decreasing survival rate [8]. Although remarkably tolerant of silt, it should be noted that higher concentrations of silt, clay, chalk, and Fuller's earth have been observed to decrease egg and larval development of the American Oyster [14]. Changes in salinity of the Bay have also been a problem: freshwater flooding has caused 90% casualty rates in areas with low salinity. Areas in the lower Bay with high salinity have been attacked by predators and diseases, whose range is determined by critical isohalines [1]. Pollution has also severely affected oysters in the James River and Rappahannock River, specifically around the

Richmond and Hampton Roads areas [1]. Dissolved oxygen levels in the Chesapeake Bay had been unstressed prior to human modification of surrounding land, but now are low, affecting the oysters' food source [11].

A shift in the manner of collecting oysters from tonging to dredging has caused a build-up of spoil areas, where layers of dead oyster shell are deposited. The latter half of the 20th century saw a 71% decrease in individuals living in spoil areas [14]. Another consequence of dredge harvesting is decrease in reef height, which has been shown to decrease the population of oysters living on said reef [8, 11].

Oysters are critical to the Bay ecosystem because of their key ability to filter the water of their estuary, thereby removing pollutants. They consume planktons, who receive their nutrients from nitrogen compounds (often in the form of nitrates and ammonia) and therefore remove these nitrogen-based compounds from the water.

However, recent repopulation efforts have experienced some success. Starting in 2004, the Army Corps of Engineers constructed oyster reefs of various heights in the Great Wicomico river. Reefs of height 25-42 cm experienced great success, with mean oyster density of 1000 per square meter. Their result was four times higher than those reefs of height 8-12 cm [8], leading us to conclude that higher reefs are more resistant to turbulence and sedimentation [8].

1.2 Model of Renewable Population and Harvesting

This paper will examine a harvesting model of oysters, considering the maturity cycle and dynamics of the oyster population itself. Our harvesting model takes into account an effort function, which can be thought of as how many boats are sent out to collect oysters. The upper bound on this function is the maximum effort the harvester is capable of applying, or the total number of boats in the fleet. Further detail regarding the effort function can be seen in following sections.

A logistic population model is sometimes used to describe a growth and harvesting

scenario, as seen in works by Clark [5] and Kot [9]. The logistic model dictates that when the population becomes too large, reproduction and survival are increasing at an unsustainable rate, thus producing a decline in population. The logistic model uses a constant effort term, signifying a fixed harvesting effort for the duration of the time period [7]. The harvesting term here, Ex, is the constant Effort multiplied by x, the population variable.

$$\frac{dx}{dt} = rx\left(1 - \frac{x}{K}\right) - Ex. \tag{1.1}$$

An alternative to a logistic constant effort model is a constant yield model. An example of this model would be a quota system: every month a fishing company catches no more than 100 tons of fish. A constant yield model could be a function of limited storage space or other constraints [7]. The constant yield equation looks very similar to the logistic model above, except the harvesting term is simply a constant, entirely determined by the Effort function and not mathematically related at all to the population.

$$\frac{dx}{dt} = rx\left(1 - \frac{x}{K}\right) - E. \tag{1.2}$$

In looking for a sustainable model that still harvests the maximum yield, we turn to the constant effort model in equation (1.1). But instead of being based upon a logistic model, our model will use a cubic growth function determined by the Allee effect.

1.3 The Allee Effect

The Allee Effect is a population dynamics model which describes the rate at which the population will increase or decrease. Its key determining factor is population density. Under the Allee Effect for large populations, reproduction and survival rates are inversely proportional to increased population density. For small populations, increased reproduction and survival rates occur as population density increases [2]. An example of Allee

Effect population growth function is

$$f(N) = rN\left(\frac{N}{K_0} - 1\right)\left(1 - \frac{N}{K}\right), \tag{1.3}$$

where the carrying capacity K is the upper bound of the population, and the minimal sustainable population K_0 is the lower bound of the population.

In his 1949 paper [2], Allee did not explicitly define the effect, but rather considered "certain aspects of survival value"[16]. Stephens et al. define the Allee Effect as "a positive relationship between any component of individual fitness and either numbers of density of conspecifics"[16]. They also distinguish between component Allee effects (manifested by a component of fitness) and demographic Allee effects (manifested at the level of total fitness). However, they do provide for negative effects of increasing population numbers, such as competition for food and over-crowding [16]. Because we examine the effect of harvesting upon the total population, we are considering a demographic Allee effect.

Shi and Shivaji studied the weak Allee Effect, in which the per capita growth rate is not as monotonically decreasing as in a logistic growth model, and the habitat is assumed to be a heterogeneously bounded region [15]. In the strong Allee Effect, the population exhibits a critical density below which the population decreases. For both the weak and strong Allee effect cases, there is a "sweet spot" at which the population is neither too small nor too big, and grows at the highest rate.

1.4 Optimal Control Theory

Optimal Control Theory describes the behavior of the underlying dynamical system (the state variable) with respect to the control function (the effort function). For the context of harvesting problems, Optimal Control Theory can be posed as a question: How do we design the control function in order to achieve our desired aims? Oftentimes, this control involves different rates of harvesting under certain conditions, determined by the cost to perform such harvesting. Consequently, we adjust the control function in order to

maximize or minimize a given objective functional [10].

Our problem is a biological application of control engineering, which seeks to apply control theory to practical systems. We change the control function in order to achieve the desired result from the response variable. In our case, we seek a stable solution during which we can harvest the maximum amount of oysters while still maintaining a sustainable, healthy population.

Optimal Control Theory has wide-ranging applications. Among other uses, it can be used to maximize commodity profit for products within a market and profits for the whole market, minimize the negative effect of pests upon a crop, optimize the productivity of an economy (theoretically, of course), or maximize return on investment [3, 12, 13, 17]. Correspondingly, the control function can take many different forms: loan rates and target prices, amount and distribution method of insecticides, pattern of consumption, or time spent by employees of an investment firm on a particular project [3, 12, 13, 17].

1.5 Review of Work for Logistic Model

Wang and Wang [18] studied the optimal harvesting strategies for a single population model in an effort very similar to ours. They use optimal control theory to study the harvesting problem with a logistic equation, in order to maximize the total yield or the terminal population. The logistic model with harvesting is represented by the population function

$$\frac{dx}{dt} = rx\left(1 - \frac{x}{K}\right) - E(t)x, \tag{1.4}$$

and they maximize the total yield over a time period $[0, T]$:

$$\int_0^T E(t)x(t)\,dt, \tag{1.5}$$

subject to (1.4), where T is the span of time of interest and $0 \leq E(t) \leq E_{max}$. Here E_{max} is the maximum effort. The resulting optimal control $E(t)$ is a Bang-Bang Control, which simply means that the effort function $E(t)$ is a Heaviside type function with value either E_{max}, 0, or an optimal effort E^* (singular value).

Wang and Wang [18] also calculate the switching times (between the different harvesting rates) T_1 and T_2 by explicit formula. This is a step that we aim to duplicate in our research for the model with strong Allee effect as well, although it may prove more difficult for us because the nonlinearity in our equation is a cubic function. T_1 here denotes the time at which $E(t)$ reaches its singular value, and T_2 denotes the time $E(t)$ leaves its singular value to resume harvesting at maximum capacity. For more detail on this process, see the discussion in Chapter 2.

1.6 Summary of Work

Our Optimal Control model finds a sustainable solution that balances oyster harvesting with the health of the population. We wish to find the value of our Effort (control) function that harvests the most oysters possible without fishing the population to extinction.

We create a Hamiltonian function and apply the Pontryagin's Maximum Principle, the basic mathematical theorem in optimal control theory [10]. Our Effort function is a Bang-Bang Control, meaning that it is a piecewise constant function where either $E(t) = 0$, $E(t) = E_{max}$, or $E(t) = E^*$ (a singular value). Much like an on-off switch, our Effort function is not continuous; it always takes one of three values. The goal is to find an E^* between 0 and E_{max} such that E^* will balance out with the natural growth rate of the population to form a constant, stable population.

Chapter 2

Mathematical Model and Analysis

2.1 Mathematical Set-up: One-Patch Model

In order to understand the dynamics of a two-patch model, we first examine the one-patch model.

We begin with equations to model the population following sources [5, 9]. Let $N(t)$ represent the population of certain species; $N(t)$ satisfies a differential equation:

$$\frac{dN(t)}{dt} = f(N(t)) - qE(t)N(t), \tag{2.1}$$

where

$$f(N) = rN\left(\frac{N}{K_0} - 1\right)\left(1 - \frac{N}{K}\right). \tag{2.2}$$

The initial condition of $N(t)$ is

$$N(0) = N_0. \tag{2.3}$$

In equation (2.1), $f(N)$ is the natural growth rate with a strong Allee effect, while $qE(t)N(t)$ represents the harvesting of the population. The Allee effect is determined by the limitation of the sustainable population value to greater than $K0$ and less than K.We

see that q is the harvesting ability, $E(t)$ is the effort put into harvesting the population, r is the intrinsic growth rate of the population, K is the carrying capacity of the population, and K_0 is the sparsity constant of the population satisfying $0 < K_0 < K$ (the minimum sustainable population value). Graphs of $f(N)$ in both a non-harvesting Allee Effect system and logistic growth model are plotted in Figure 2.1. From the Allee Effect graph, it is clear that if $N_0 < K_0$, the solution approaches 0, but if $N_0 > K_0$ then the solution approaches K. However, in the logistic case, a solution with $N_0 > 0$ always approaches K.

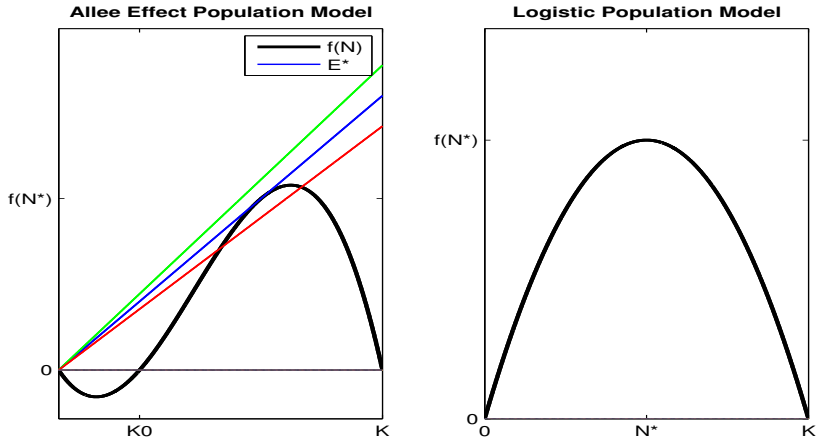

Figure 2.1: Graph of $f(N)$ for a population following the Allee Effect (left) and one with logistic growth (right). For this graph, $K = 20$, $K_0 = 5$, and $r = 1$.

In order to define the best effort function $E(t)$, we employ dynamic optimization. Our goal is to maximize

$$\int_0^T pqE(t)N(t)\,dt \tag{2.4}$$

subject to (2.1) and $0 \leq E(t) \leq E_{max}$, where E_{max} is the maximum possible harvesting effort, p is the value per unit harvested and T is the total time of interest. Through this process, we define a Hamiltonian function

$$H(N(t), E(t), \lambda(t)) = pqE(t)N(t) + \lambda(t)[f(N(t)) - qE(t)N(t)], \tag{2.5}$$

where $\lambda(t)$ is a scalar function of t. The Hamiltonian can be rewritten as

$$H(N(t), E(t), \lambda(t)) = [p - \lambda(t)]qE(t)N(t) + \lambda(t)f(N(t)). \tag{2.6}$$

By Pontryagin's Maximum Principle [9, page 243], we can conclude that the following equations are satisfied by the optimal control $E(t)$ and corresponding $N(t)$ and $\lambda(t)$:

$$\begin{cases} \dfrac{dN}{dt} = \dfrac{\partial H}{\partial \lambda} = f(N) - qEN, \\ \dfrac{d\lambda}{dt} = -\dfrac{\partial H}{\partial N} = -q(p - \lambda)E - \lambda f'(N), \\ N(0) = N_0, \quad \lambda(T) = 0. \end{cases} \tag{2.7}$$

In the Hamiltonian (2.6), we can consider $N(t)$ a known quantity because it is our state variable, and focus our energies on the control function $E(t)$. Thus we treat $N(t)$ as a constant, and consider maximizing $H(t)$ with a given $\lambda(t)$. Then $E(t)$ has to satisfy

$$E(t) = \begin{cases} E_{max}, & \lambda(t) < p, \\ E^*, & \lambda(t) = p, \\ 0, & \lambda(t) > p. \end{cases} \tag{2.8}$$

where $E^* < E_{max}$ is to be specified. This E^* is the optimal effort value, which is the maximum sustainable effort value that does not drive the population to extinction. Such a piecewise constant effort function is called a bang-bang control (see Fig. 2.2). In a bang-bang control situation, E^* is called a singular value.

In order to obtain E^*, we examine the situation in which $\lambda(0) = p$. If $\lambda(t) = p$ over an interval, $\dfrac{d\lambda}{dt}$ becomes zero, as does the term $-q(p-\lambda)E$. So, we know (because $\lambda = p$) that $f'(N)$ must equal zero as well. Therefore, the $\dfrac{dN}{dt}$ term of equation (2.7) is zero. Hence, we can obtain an N^* by solving $f'(N^*) = 0$. Notice that for the strong Allee effect $f(N)$, there are two N-values such that $f'(N) = 0$. But the smaller one satisfies $f(N) < 0$, which will drive the population to extinction because it is an unstable solution.

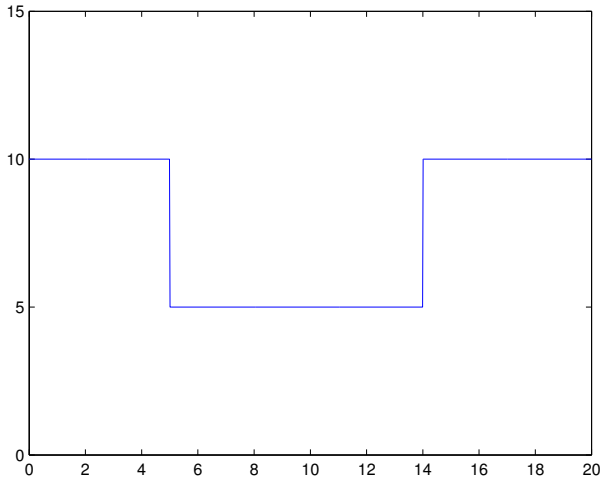

Figure 2.2: A Bang-Bang Control $E(t)$ with $E_{max} = 10$ and $E^* = 5$.

Hence we choose the larger one. Once we have N^*, we obtain E^* by solving the remaining parts of equation (2.7) for E:

$$E^* = \frac{f(N^*)}{qN^*}.$$

We first solve for N^*.

$$0 = f'(N) = \frac{r}{KK_0}(-3N^2 + 2(K + K_0)N - K_0K), \tag{2.9}$$

$$0 = -3N^2 + 2(K + K_0)N - K_0K. \tag{2.10}$$

Now we apply the quadratic formula to obtain:

$$N = \frac{2(K + K_0) \pm \sqrt{4(K + K_0)^2 - 12KK_0}}{6}, \tag{2.11}$$

$$N = \frac{K + K_0 \pm \sqrt{K^2 - KK_0 + K_0^2}}{3}. \tag{2.12}$$

We know we must pick the root of this equation with the positive sign, because the root with the negative sign drives the solution to zero. Hence

$$N^* = \frac{K + K_0 + \sqrt{K^2 - KK_0 + K_0^2}}{3}. \tag{2.13}$$

Now that we know N^*, we can solve for E^*:

$$E^* = \frac{f(N^*)}{qN^*} = \frac{r}{qKK_0}\left[-(N^*)^2 + (K + K_0)N^* - K_0K\right]. \tag{2.14}$$

But we know that

$$(N^*)^2 = \frac{2(K + K_0)N^* - K_0K}{3}. \tag{2.15}$$

So,

$$E^* = \frac{r}{qKK_0}\left[\left(-\frac{2(K + K_0)N^* - K_0K}{3}\right) + (K + K_0)N^* - K_0K\right], \tag{2.16}$$

$$E^* = \frac{r}{qKK_0}\left[\frac{1}{3}(K + K_0)N^* - \frac{2}{3}K_0K\right], \tag{2.17}$$

$$E^* = \frac{r}{qKK_0}\left[\frac{1}{9}(K + K_0)\left(K + K_0 + \sqrt{K^2 - KK_0 + K^2}\right) - \frac{2}{3}K_0K\right]. \tag{2.18}$$

With the values $r = 1$, $q = 1$, $K_0 = 5$ and $K = 20$ in equations (2.13) and (2.18), we obtain the values $N^* = 14.3426$ and $E^* = 0.52855$. Under this particular example of harvesting effort, the solution of the state equation would look like Figure 2.3, in which we take $E(t) = E^* = 0.52855$. Solving $(1 - N/K)(N/K_0 - 1) - E^* = 0$, we obtain two roots $N_1 = 10.6574$ and $N_2 = 14.3426$, which will be the asymptotes of solutions depending upon initial values. If $N_0 > N_1$, the solution for the system would follow the top trend line to approach N_2, whereas if $0 < N_0 < N_1$, the solution would trend to zero. Here the singular value N^* is same as the upper equilibrium N_2, which occurs because $q = 1$.

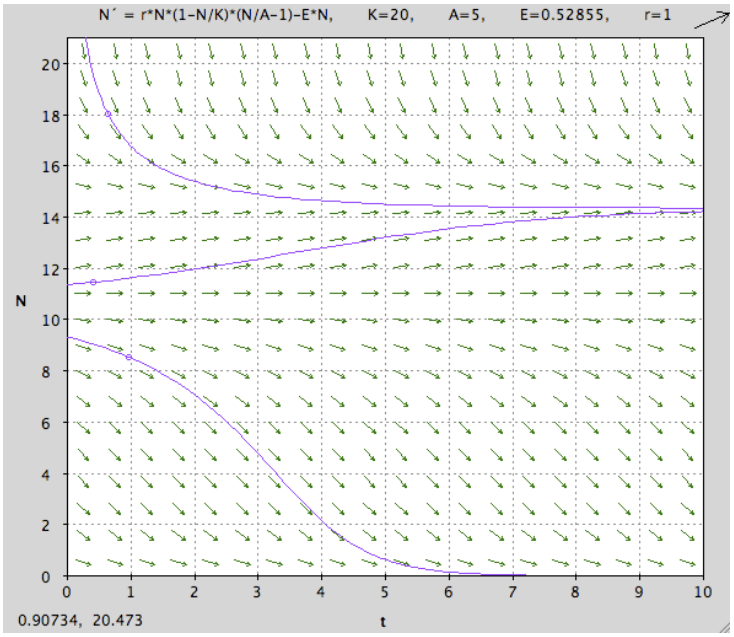

Figure 2.3: Direction field showing solutions for possible initial values N_0. Here the horizontal axis is time t, and the vertical axis is $N(t)$. We use $r = 1$, $q = 1$, $K_0 = 5$, $K = 20$ and $E = 0.52855$.

The effort function for the system is a piecewise constant function with values 0, E_{max}, or E^*; possible cases for the graph of $E(t)$ are displayed in Figures 2.4 and 2.5. In Figure 2.4, the initial condition N_0 is less than the optimal sustainable population level N^*, so the initial harvesting effort is set to zero in order to allow the population to grow to reach N^*. In Figure 2.5, N_0 is greater than N^*, allowing the initial harvesting level to be $E(t) = E_{max}$ in order to reduce the population to sustainable level N^*. However, to determine more precisely when to switch to a particular value of $E(t)$, we explicitly construct the optimal solution for the system in Section 2.2. We will also solve specifically for the state-switching times T_1 and T_2.

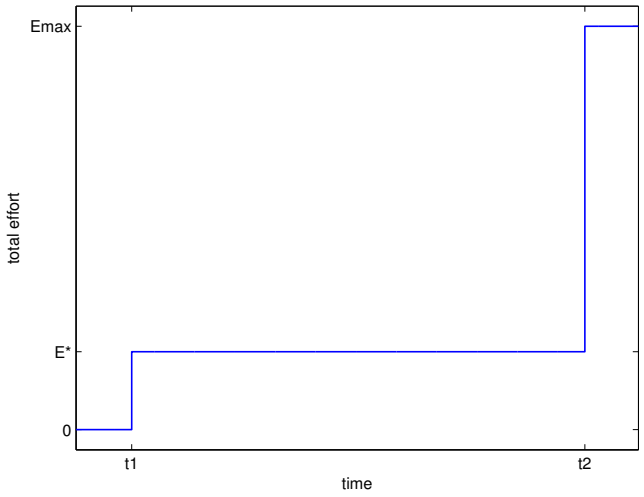

Figure 2.4: A possible $E(t)$ over time for $N_0 < N^*$.

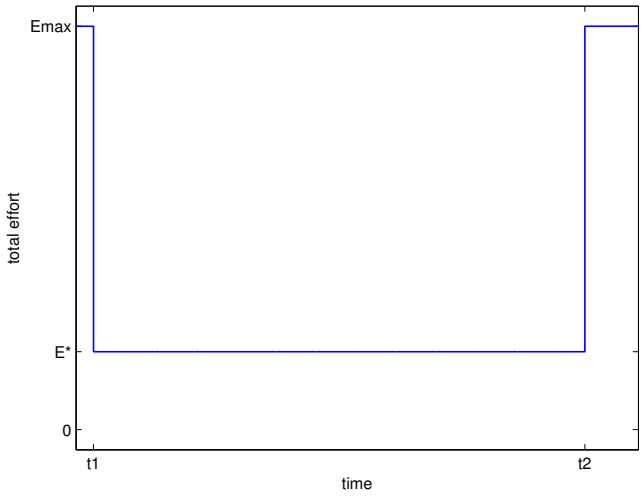

Figure 2.5: A possible $E(t)$ over time for $N_0 > N^*$.

2.2 Optimal Solution

From the bang-bang control theory, for a large T, the optimal solution may take two forms.

2.2.1 Case 1: $K_0 < N_0 < N^*$

In order to find the optimal solution of this problem, we must solve the population equation. However, we must consider two cases: $K_0 < N_0 < N^*$ and $N_0 > N^*$. We first tackle $K_0 < N_0 < N^*$. In this case we first set the effort to $E = 0$ so the population can recover to the level of singular value E^*. We integrate the differential equation in this case:

$$\frac{dN}{dt} = rN\left(\frac{N}{K_0} - 1\right)\left(1 - \frac{N}{K}\right), \tag{2.19}$$

$$\int \frac{dN}{N(K-N)(N-K_0)} = \int \frac{r}{KK_0} dt, \tag{2.20}$$

$$\int \left(\frac{1}{K_0(K-K_0)}\frac{1}{N-K_0} - \frac{1}{K(K-K_0)}\frac{1}{N-K} - \frac{1}{KK_0N}\right) dN = \int \frac{r}{KK_0} dt, \tag{2.21}$$

$$\ln|N-K_0|^k - \ln|N-K|^{K_0} - (K-K_0)\ln(N)^{K-K0} = r(K-K_0)t + C, \tag{2.22}$$

$$\frac{|N-K_0|^K}{|N-K|^{K_0}N^{K-K_0}} = Ce^{r(K-K_0)t}. \tag{2.23}$$

From $N(0) = N_0$, we have

$$\frac{|N_0-K_0|^K}{|N_0-K|^{K_0}N_0^{K-K_0}} = C. \tag{2.24}$$

This gives the final equation, which allows us to later solve for T_1:

$$\frac{|N-K_0|^K}{|N-K|^{K_0}N^{K-K_0}} = \frac{|N_0-K_0|^K}{|N_0-K|^{K_0}N_0^{K-K_0}}e^{r(K-K_0)t}. \tag{2.25}$$

Solving for T_1 we obtain:

$$\ln\left(\frac{|N^*-K_0|^K}{|N^*-K|^{K_0}(N^*)^{K-K_0}}\right) = \ln\left(\frac{|N_0-K_0|^K}{|N_0-K|^{K_0}N_0^{K-K_0}}\right) + r(K-K_0)T_1, \tag{2.26}$$

$$T_1 = \frac{1}{r(K-K_0)}\left(\ln\left(\frac{|N^*-K_0|^K}{|N^*-K|^{K_0}(N^*)^{K-K_0}}\right) - \ln\left(\frac{|N_0-K_0|^K}{|N_0-K|^{K_0}N_0^{K-K_0}}\right)\right), \tag{2.27}$$

and, finally,

$$T_1(N_0) = \frac{1}{r(K-K_0)}\left(\ln\left(\frac{|N^*-K_0|^K}{|N^*-K|^{K_0}(N^*)^{K-K_0}} * \frac{|N_0-K|^{K_0}N_0^{K-K_0}}{|N_0-K_0|^K}\right)\right). \tag{2.28}$$

A graph of $T_1(N_0)$ is given in Figure 2.6. Biologically, $T_1(N_0)$ in equation (2.28) gives a recovery time for the fishery from a lower stock level to an optimal stock level N^*, which maximizes the harvest. Clearly this recovery time is longer when N_0 is farther from N^*. In this case, when $N_0 < N^*$, the time T_1 is a "waiting time" for the fisherman before he can begin harvesting.

2.2.2 Case 2: $N_0 > N^*$

Next, we consider the case where the initial population value, N_0, is greater than N^*. If this is the case, then our prior formulas do not apply because they lack a harvesting term. The bang-bang control suggests that a maximal harvesting effort E_{max} is taken until $N(t)$ reaches N^*. Hence we consider the differential equation

$$\frac{dN}{dt} = rN\left(\frac{N}{K_0}-1\right)\left(1-\frac{N}{K}\right) - E_{max}N. \tag{2.29}$$

Integrating equation (2.29) we obtain

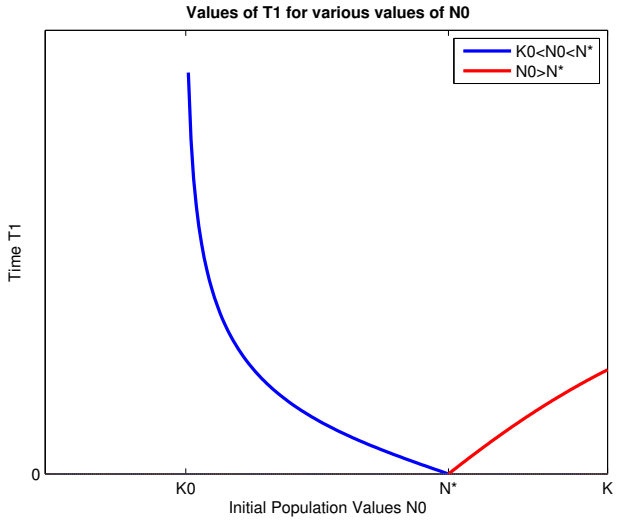

Figure 2.6: Values for T_1 for various values of N_0, where $r = 1$, $N^* = 14.3426$, $K_0 = 5$ and $K = 20$.

$$\int \frac{dN}{N(K-N)(N-K_0) - E_{max}KK_0N} = \int \frac{r}{KK_0}dt. \tag{2.30}$$

Here, to reduce the complexity of the equations, we define variable $A = E_{max}KK_0$. Employing the method of partial fractions, we have

$$\int \frac{a}{N}dN + \int \frac{bN+c}{(K-N)(N-K_0) - A}dN = \int \frac{r}{KK_0}dt. \tag{2.31}$$

The quadratic form $(K-N)(N-K_0)-A$ has no real roots because of the choice of E_{max}. We now solve for the coefficients a, b and c:

$$a(-N^2 + (KK_0)N - KK_0 - A) + bN^2 + cN = 1. \tag{2.32}$$

Thus

$$\begin{aligned} -a + b &= 0, \\ a(K + K_0) + c &= 0, \\ -a(KK_0 + A) &= 1, \end{aligned} \tag{2.33}$$

and we obtain the values

$$\begin{aligned} a &= \frac{-1}{KK_0 + A}, \\ b &= \frac{1}{KK_0 + A}, \\ c &= \frac{K + K_0}{KK_0 + A}. \end{aligned} \tag{2.34}$$

We now must complete the square of the denominator of this integral in order to integrate it:

$$\int \frac{a}{N} dN + \int \frac{bN + c}{(N - \frac{K+K_0}{2})^2 + KK_0 + A - \frac{(K+K0)^2}{4}} dN = \int \frac{r}{KK_0} dt, \tag{2.35}$$

$$\int \frac{a}{N} dN + \int \frac{bN + c}{\left(N - \frac{K+K_0}{2}\right)^2 + KK_0 + A - \frac{(K+K_0)^2}{4}} dN = \int \frac{r}{KK_0} dt, \tag{2.36}$$

$$\int \frac{a}{N} dN + \int \frac{b(N - \frac{K+K_0}{2}) + c + \frac{b(K+K_0)}{2}}{\left(N - \frac{K+K_0}{2}\right)^2 + A - \frac{(K-K_0)^2}{4}} dN = \int \frac{r}{KK_0} dt. \tag{2.37}$$

The next step is another change of variable, defining $W = N - \frac{K+K_0}{2}$ and $A_1^2 = A - (\frac{K-K_0}{2})^2$. Then, the above integral becomes

$$\int \frac{a}{N} dN + \int \frac{bW}{W^2 + A_1^2} dW - \int \frac{c + \frac{b(K+K_0)}{2}}{W^2 + A_1^2} dW = \int \frac{r}{KK_0} dt. \tag{2.38}$$

Now the integration can be done, so we have

$$a \ln N - \frac{b}{2} \ln \left(W^2 + A - \left(\frac{KK_0}{2} \right)^2 \right) - \frac{c + \frac{b(K+K_0)}{2}}{A_1} \tan^{-1} \frac{W}{A_1} = \frac{r}{KK_0} t + C. \tag{2.39}$$

Substituting the original variables back into the equation:

$$\begin{aligned}
&-\frac{1}{KK_0(1+qE_{max})}\ln N \\
&-\frac{1}{2KK_0(1+qE_{max}KK_0)}\ln\left(N^2-(K_0+K)N+KK_0(1+qE_{max})\right) \\
&-\frac{\frac{K+K_0}{KK_0(1+qE_{max})}+\frac{K+K_0}{2KK_0(1+qE_{max})}}{\sqrt{qE_{max}KK_0-(\frac{K-K_0}{2})^2}}\tan^{-1}\left(\frac{N-\frac{K+K_0}{2}}{\sqrt{qE_{max}KK_0-(\frac{K-K_0}{2})^2}}\right) \\
=&\frac{r}{KK_0}t+C.
\end{aligned} \tag{2.40}$$

Multiplying both sides of the equation by $-KK_0(1+qE_{max})$, we obtain

$$\begin{aligned}
&\ln N+\frac{1}{2}\ln\left(N^2-(K_0+K)N+KK_0+qE_{max}KK_0\right) \\
&+\frac{3(K+K_0)}{2\sqrt{qE_{max}KK_0-(\frac{K-K_0}{2})^2}}\tan^{-1}\left(\frac{N-\frac{K+K_0}{2}}{\sqrt{qE_{max}KK_0-(\frac{K-K_0}{2})^2}}\right)=-rt(1+qE_{max})+C.
\end{aligned} \tag{2.41}$$

Now, we set $t=0$ and $N(0)=N_0$ to solve for the constant C.

$$\begin{aligned}
C=&\ln N_0+\frac{1}{2}\ln\left(N_0^2-(K_0+K)N_0+KK_0+qE_{max}KK_0\right) \\
&+\frac{3(K+K_0)}{2\sqrt{qE_{max}KK_0-(\frac{K-K_0}{2})^2}}\tan^{-1}\left(\frac{N_0-\frac{K+K_0}{2}}{\sqrt{qE_{max}KK_0-(\frac{K-K_0}{2})^2}}\right).
\end{aligned} \tag{2.42}$$

When $t=T_1$, $N=N^*$, so we reach a formula for T_1 for the case of $N_0>N^*$:

$$T_1(N_0) = \frac{-1}{r(1+qE_{max}KK_0)}\Bigg[\ln N^* + \frac{1}{2}\ln\left((N^*)^2 - (K_0+K)N + KK_0 + qE_{max}KK_0\right)$$
$$+ \frac{3(K+K_0)}{2\sqrt{qE_{max}KK_0 - (\frac{K-K_0}{2})^2}}\tan^{-1}\left(\frac{N^* - \frac{K+K_0}{2}}{\sqrt{qE_{max}KK_0 - (\frac{K-K_0}{2})^2}}\right)$$
$$- \ln N_0 + \frac{1}{2}\ln\left(N_0^2 - (K_0+K)N_0 + KK_0 + qE_{max}KK_0\right)$$
$$+ \frac{3(K+K_0)}{2\sqrt{qE_{max}KK_0 - (\frac{K-K_0}{2})^2}}\tan^{-1}\left(\frac{N_0 - \frac{K+K_0}{2}}{\sqrt{qE_{max}KK_0 - (\frac{K-K_0}{2})^2}}\right)\Bigg]. \tag{2.43}$$

Again, a graph of $T_1(N_0)$ is shown in Figure 2.6. One can see that $T_1(N_0)$ for $N_0 > N^*$ is almost linear while $T_1(N_0)$ for $K_0 < N_0 < N^*$ has a vertical asymptote at $N = K_0$. Biologically, the $T_1(N_0)$ shows the maximal time length that maximum harvesting is allowed if initially the oyster stock is abundant, while refraining from driving the stock to a dangerously low state. Hence this T_1 represents a "bountiful harvest time" for the fisherman during which he does not need to worry about the sustainability of the population.

2.2.3 Solving for T_2

T_2 is defined as the time at which the harvesting effort changes from E^* back to E_{max}, and remains at E_{max} until the end of time T. When solving for T_2, we must include the equation for $\lambda(t)$ because of the transversality condition of Pontryagin's Maximum Principle: $\lambda(T) = 0$. Hence we consider the following differential equations:

$$\frac{dN}{dt} = rN\left(\frac{N}{K_0} - 1\right)\left(1 - \frac{N}{K}\right) - qE_{max}N, \tag{2.44}$$

$$\frac{d\lambda}{dt} = -q(p-\lambda)E_{max} - \lambda\frac{r}{KK_0}(-3N^2 + 2N(K+K_0) - KK_0), \tag{2.45}$$

with initial and terminal conditions

$$\begin{cases} N(T_2) = N^*, \\ \lambda(T_2) = p, \\ \lambda(T) = 0. \end{cases} \tag{2.46}$$

The equation of N is solved by equations (2.41) and (2.42), with the one exception that in equation (2.42), N_0 is replaced by N^*, to form the following two equations:

$$\begin{aligned} &\ln N + \frac{1}{2}\ln\left(N^2 - (K_0+K)N + KK_0 + qE_{max}KK_0\right) \\ &+ \frac{3(K+K_0)}{2\sqrt{qE_{max}KK_0 - (\frac{K-K_0}{2})^2}} \tan^{-1}\left(\frac{N - \frac{K+K_0}{2}}{\sqrt{qE_{max}KK_0 - (\frac{K-K_0}{2})^2}}\right) = -rt(1+qE_{max}) + C, \end{aligned} \tag{2.47}$$

$$\begin{aligned} C = &\ln N^* + \frac{1}{2}\ln\left((N^*)^2 - (K_0+K)N^* + KK_0 + qE_{max}KK_0\right) \\ &+ \frac{3(K+K_0)}{2\sqrt{qE_{max}KK_0 - (\frac{K-K_0}{2})^2}} \tan^{-1}\left(\frac{N^* - \frac{K+K_0}{2}}{\sqrt{qE_{max}KK_0 - (\frac{K-K_0}{2})^2}}\right). \end{aligned} \tag{2.48}$$

We then substitute this expression of N into equation (2.45), which is a linear differential equation. An analytical solution is possible, but due to the incredibly complex nature of this calculation we will not include it here. However, we are able to solve for T_2 using a numerical method to solve the equation of $\lambda(t)$. Biologically during the final period $[T_2, T]$, fishermen do not pay attention to the population level, but only try to maximize the total harvesting. This is because they only try to maximize the harvesting for a finite time period $[0, T]$, not beyond T. So in reality, this T_2 is not so important: we really should set $T = \infty$ so the ecosystem can be in a healthy state forever.

2.2.4 Summary of Optimal Solution

In summary, in order to find T_1, there are two cases. If $K_0 < N_0 < N^*$, then we use equation (2.28), when $N = N^*$. If $N_0 > N^*$, we use equation (2.47).

In Figure 2.7 and Figure 2.8, the graphs of the effort, population, and lambda functions for the entire range $[0, T]$ are plotted using `Matlab` simulation.. The graphs for $N_0 > N^*$ is shown in Fig. 2.7, and the graphs for $K_0 < N_0 < N^*$ is shown in Fig. 2.8. Both figures use parameters $K_0 = 5$, $K = 20$, $r = 1$, $q = 1$, $p = 0.5$, and $T = 3$.

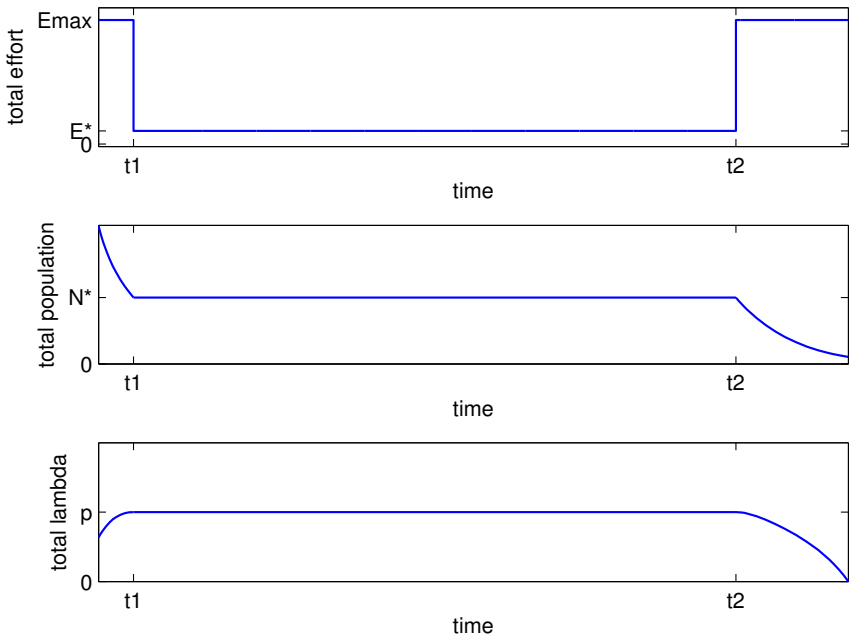

Figure 2.7: Graphs of effort, population, and lambda for time T and $N_0 > N^*$. Values for the parameters are $N_0 = 30$, $\lambda_0 = \lambda(0) = 0.3165$, and $E_{max} = 5$. The changes in $E(t)$ take place at $T_1 = 0.1399$ and $T_2 = 2.5502$.

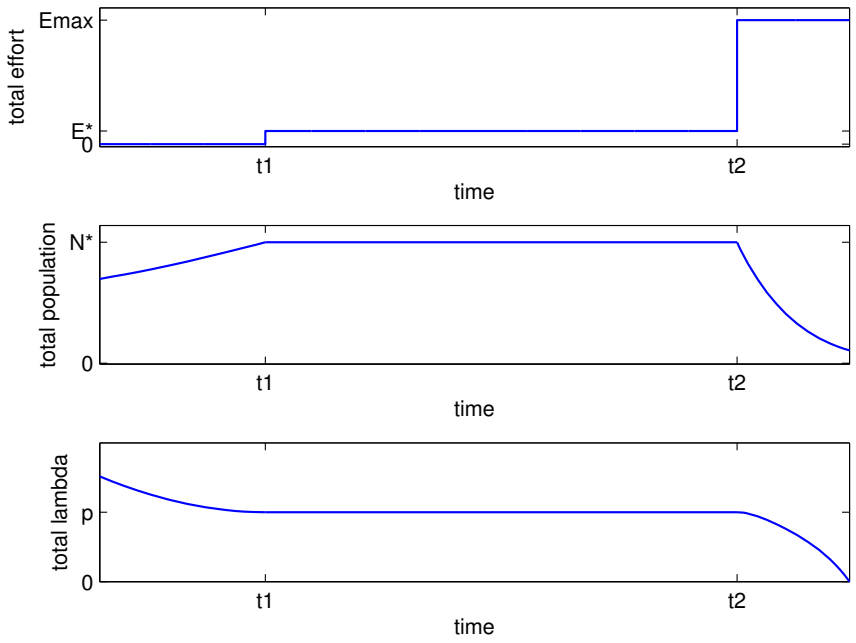

Figure 2.8: Graphs of effort, population, and lambda for time T and $N_0 < N^*$. Values for the parameters are $N_0 = 10$, $\lambda_0 = \lambda(0) = 0.758$, and $E_{max} = 5$. The changes in $E(t)$ take place at $T_1 = 0.6628$ and $T_2 = 2.5502$.

See Section 5.1 for our One Patch Program.

2.3 Two-Patch Model

The obvious extension of the one-patch model described above is a two-patch model consisting of two models that exhibit the same behavior. We can begin the same process as above, and the populations in the two patches satisfy:

$$\frac{dN_1}{dt} = f(N_1(t)) - qE_1(t)N_1(t), \tag{2.49}$$

$$\frac{dN_2}{dt} = f(N_2(t)) - qE_2(t)N_2(t), \tag{2.50}$$

$$\begin{cases} N_1(0) = N_{10}, \\ N_2(0) = N_{20}, \end{cases} \tag{2.51}$$

where:

$$f(N_i) = rN_i\left(\frac{N_i}{K_0} - 1\right)\left(1 - \frac{N_i}{K}\right). \tag{2.52}$$

So, we must maximize the following integral:

$$\int_0^T pq[E_1(t)N_1(t) + E_2(t)N_2(t)]\,dt, \tag{2.53}$$

where $0 \leq E_1 \leq E_{max}$ and $0 \leq E_2 \leq E_{max}$.

The integral is optimized subject to equations (2.49) and (2.50). We then repeat the process of constructing the Hamiltonian:

$$H = pq(E_1N_1 + E_2N_2) + \lambda_1(t)[f(N_1) - qE_1N_1] + \lambda_2(t)[f(N_2) - qE_2N_2]. \tag{2.54}$$

By Pontryagin's Maximum Principle, we obtain the system of equations

$$\begin{cases} \dfrac{dN_1}{dt} = f(N_1) - qE_1N_1, \\ \dfrac{dN_2}{dt} = f(N_2) - qE_2N_2, \\ \dfrac{d\lambda_1}{dt} = \dfrac{-\partial H}{\partial N_1} = -pqE_1 - \lambda_1[f'(N_1) - qE_1], \\ \dfrac{d\lambda_2}{dt} = \dfrac{-\partial H}{\partial N_2} = -pqE_2 - \lambda_2[f'(N_1) - qE_2], \\ N_1(0) = N_{10}, \\ N_2(0) = N_{20}, \\ \lambda_1(T) = 0, \\ \lambda_2(T) = 0. \end{cases} \tag{2.55}$$

Equation (2.54) can be re-arranged into the following version of the Hamiltonian:

$$H = [p - \lambda_1(t)]qE_1N_1 + [p - \lambda_2(t)]qE_2N_2 + \lambda_1 f(N_1) + \lambda_2 f(N_2). \tag{2.56}$$

According to equation (2.56), we can again hypothesize the three possible ranges for $E_i(t)$:

$$E_i(t) = \begin{cases} E_{max}, & \lambda_i(t) < p, \\ E^*, & \lambda_i(t) = p, \\ 0, & \lambda_i(t) > p. \end{cases} \tag{2.57}$$

Because of the variation in the values of $\lambda_i(t)$, there are several options for each effort function $E_i(t)$. Figure 2.9, Figure 2.10, and Figure 2.11 below are just three of the four possible scenarios, based upon independent $E_i(t)$. I have not included the graph for the case in which $E_{10} < E_1^*$ and $E_{20} > E_2^*$.

In order to analyze the independently-harvested two-patch scenario, we use largely the same process as the one-patch scenario. We can apply Pontryagin's Maximum Principle and analyze the Hamiltonian in the same manner, and derive the same relationship between p, λ, and $E(t)$. More intricate scenarios, such as dependent effort functions and dispersion between patches, present intriguing projects to consider for future work.

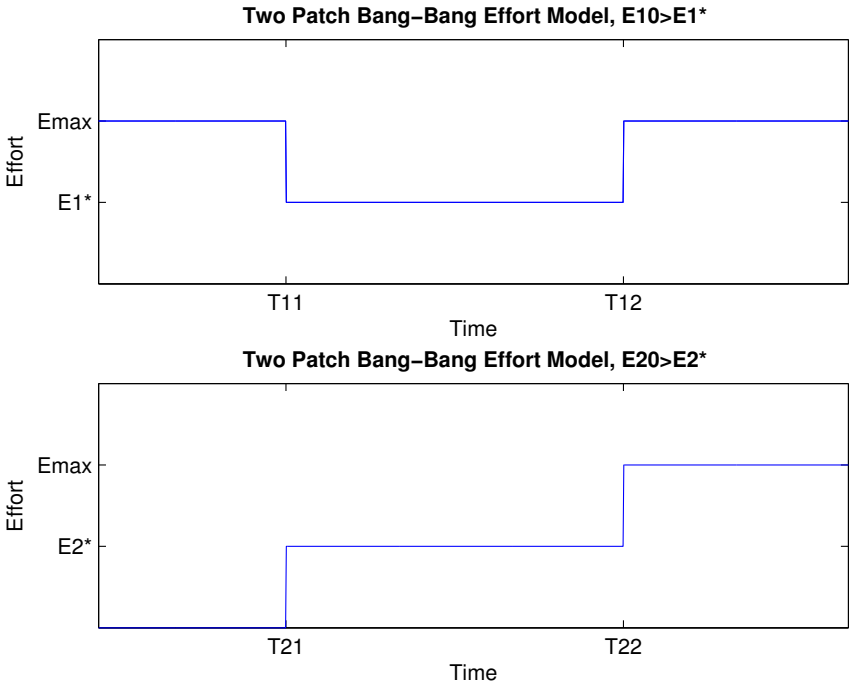

Figure 2.9: $E(t)$ while using Bang-Bang Control, $E_{10} > E_1^*$, $E_{20} < E_2^*$.

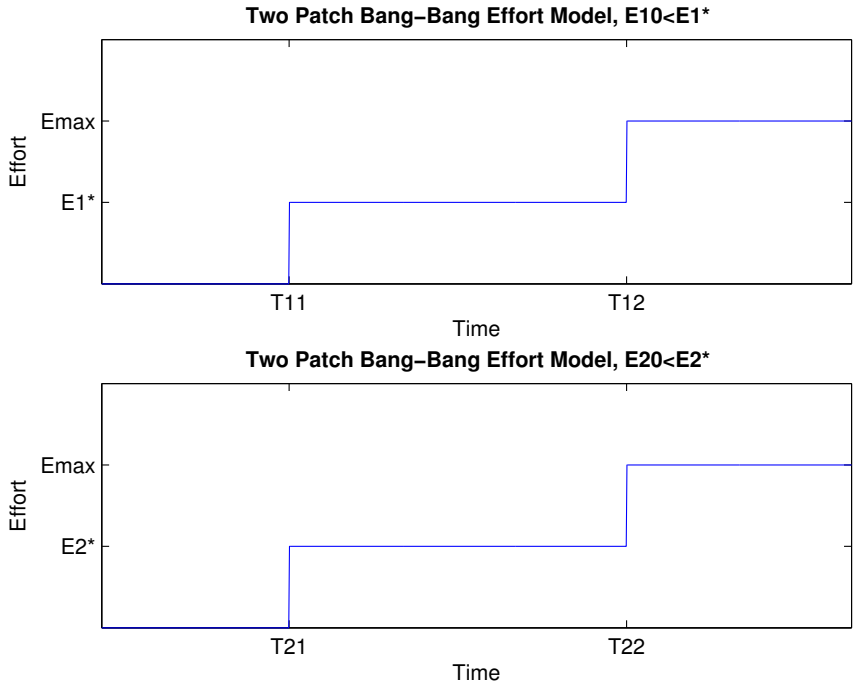

Figure 2.10: $E(t)$ while using Bang-Bang Control, $E_{10} < E_1^*$, $E_{20} < E_2^*$.

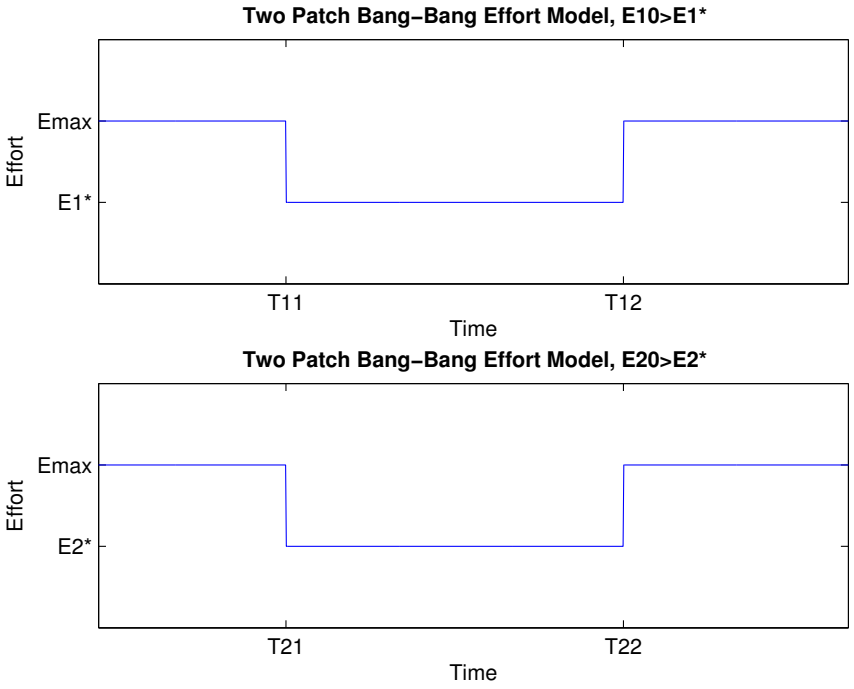

Figure 2.11: $E(t)$ while using Bang-Bang Control, $E_{10} > E_1^*$, $E_{20} > E_2^*$.

Chapter 3

Numerical Simulations

3.1 Review of the Forward-Backward Sweeping Algorithm

The Forward-Backward Sweeping Algorithm is a numerical method intended to generate a very close approximation to the analytical solution of our model. It is an example of a block Gauss-Seidel fixed-point iteration.

We must maximize

$$\int_0^T pqE(t)N(t)\,dt \tag{3.1}$$

subject to

$$\frac{dN}{dt} = f(N(t)) - qE(t)N(t), \tag{3.2}$$

and $0 \leq E(t) \leq E_{max}$. As we saw in Section 2.1, the solution to the above optimal control problem must also satisfy the equations following below [10]:

$$\frac{dN}{dt} = \frac{\partial H}{\partial \lambda} = f(N) - qEN, \quad N(0) = N_0, \tag{3.3}$$

$$\frac{d\lambda}{dt} = -\frac{\partial H}{\partial N} = -q(p-\lambda)E - \lambda f'(N), \quad \lambda(T) = 0, \tag{3.4}$$

$$0 = \frac{\partial H}{\partial E} = (p - \lambda(t))qN \tag{3.5}$$

The following steps are required to execute this method [10]:

Step 1. Make an initial guess for $E(t)$ over the interval $[0, T]$.

Step 2. Using the initial condition $N(0) = N_0$ and the values for $E(t)$, solve $N(t)$ forward in time according to its differential equation in the optimality system.

Step 3. Using the transversality condition $\lambda(T) = 0$ and the values for $E(t)$ and $N(t)$, solve $\lambda(t)$ backward in time according to its differential equation in the optimality system.

Step 4. Update $E(t)$ by entering the new $N(t)$ and $\lambda(t)$ values into the characterization of the optimal control.

Step 5. Check convergence. If the values of the variables in this iteration and the last iteration are negligibly close, output the current values as solutions. If the values are not close, return to Step 2.

3.2 Numerical Results for the One-Patch Model

The intent of the numerical simulation is to provide a visual representation of the ideal analytical solution to our equations. We want the graphs of our analytical solution to match those of the numerical solution, so as to confirm that our derivation of equations, programming, and graphical representations are as accurate as possible. The numerical simulation is yet another way of confirming the exactitude of our analysis in order to make factual conclusions.

For our particular case, we ran the numerical simulation with the following values:

$K_0 = 5$

$K = 20$

$r = 1$

$q = 1$

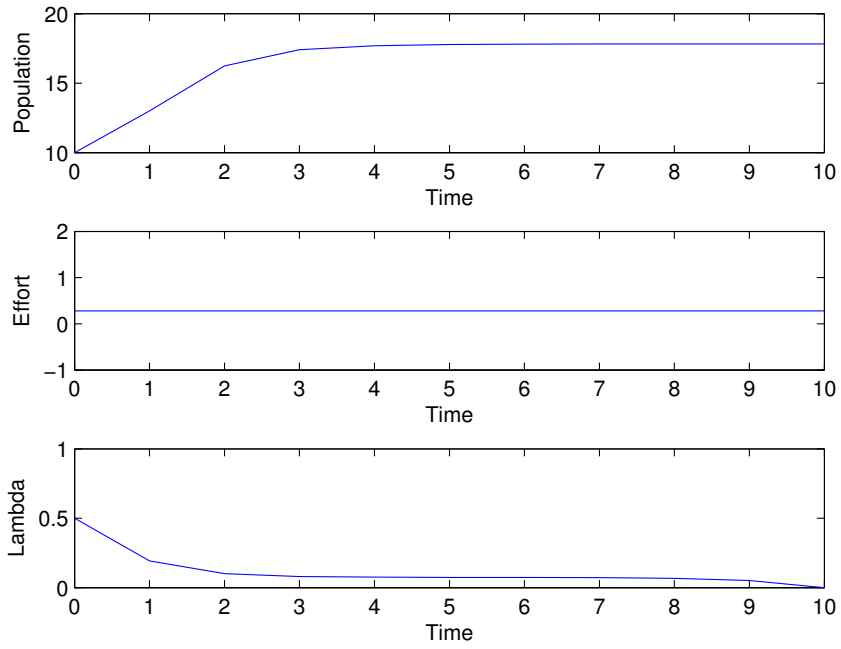

Figure 3.1: Forward-Backward Sweeping Runge-Kutta Algorithm $K_0 = 5, K = 20, r = 1, q = 1, p = 0.5, N_0 = 10, E_{max} = 0.27907, T = 10$.

$p = 0.5$

$N_0 = 10$

$E_{max} = 2$

$T = 10$.

Equations (3.1) and (3.2) were discretized using a fourth order explicit Runge-Kutta simulation. See Section 5.2 for our code, which ran many iterations of the simulation in order to produce and graph results. The graph of our numerical approximation of the equations is displayed below.

The sweeping program works for the program in Lenhart's book [10], but when adapting the program to our problem there is a convergence issue. The Forward-Backward Sweeping Runge-Kutta approximation is not guaranteed to converge for all systems, and

we found out through much trial and error that our system ($K0 = 5, K = 20, r = 1, q = 1, p = 0.5, N_0 = 10, T = 10$) only converges when $0 \leq E_{max} \leq 0.27907$. When the aforementioned parameters are used, the algorithm converges, but if the values are adjusted just slightly the algorithm no longer converges.

It is possible that this constant, 0.27907, is some combination of the rest of the parameters and forms an asymptote. As soon as the value for E_{max} becomes greater than 0.27907, the simulation no longer converges; instead, it diverges to infinity. By looking at the graph of the values, we see that the graph of $E(t)$ does not exhibit the Heaviside characteristics of a typical bang-bang control variable. Instead, $E(t)$ is constant for the duration of time T. According to Equations (2.13) and (2.17), we can calculate that, with the above parameters, $E^* = 0.5285$. Because $E_{max} = 0.27907$ is smaller than $E^* = 0.5285$, logic of the bang-bang Control dictates that there is no need to switch to the larger value E^* since one could maintain harvesting at the maximum value. Consequently, the effort function is displayed as constant, rather than the piecewise heaviside function in previous situations.

The initial and terminal conditions of $\lambda(t)$ are satisfied in the above graph as well. It is apparent that $\lambda(0) = 0.5$, which is the parameter as entered in the program, and $\lambda(T) = 0$ as declared in the terminality condition of Pontryagin's Maximum Principle in equation (2.7). Also, the behavior of the population $N(t)$ corresponds to the constancy of E_{max}, and continues to increase at a decreasing rate until time T.

Chapter 4

Conclusions

4.1 Limitations

Our model has several limitations. The first concerns the robustness of our model. Our system of equations deals with a very specific set of circumstances depicted by solvable integrals, which only occur in nature with very limited frequency. If some external factors lead to a specific population not exhibiting the Allee Effect but which was instead described by a Logistic Growth, Beverton-Holt, or Ricker model, our system of equations and solutions would not apply. Instead, the same process would have to be repeated with the population equation of the pertinent model.

Another application of optimal control theory, instead of maximizing harvesting, includes economic factors allowing for maximization of profit. Our model does not include the necessary terms to address this problem. However, the modification to the equations is not difficult [9]:

$$\max_{0 \leq E(t) \leq E_{max}} \int_0^T e^{-\delta t} E(t) N(t) dt + p e^{-\delta t} N(t), \tag{4.1}$$

subject to

$$\frac{dN}{dt} = rN\left(\frac{N}{K_0} - 1\right)\left(1 - \frac{N}{K}\right) - EN. \tag{4.2}$$

Here δ is the rate at which the economic rent is discounted. The inclusion of this term isn't strictly for the maximization of profit; it indicates that the harvester values the present harvest over future harvest. We can also incorporate an operating cost c:

$$\max_{0 \leq E(t) \leq E_{max}} \int_0^T e^{-\delta t}[pqN(t) - c]E(t)dt, \tag{4.3}$$

subject to

$$\frac{dN}{dt} = f(N) - qEN. \tag{4.4}$$

The inclusion of these possible modifications that address shortfalls of our model could provide a foundation for future work.

4.2 Future Work

In addition to the economic factors discussed above, several possible paths for future work revolve around the two patch construction. Time restrictions dictated that our work on the two-patch model not foray into co-dependent patches. However, this topic appears to be quite interesting and complex, with great applications in marine conservation efforts. There are two main ways in which oyster patches can be co-dependent:

1. The harvester shares the same harvesting resources between the two patches.

2. There is dispersion between the two oyster patches.

The subsequent sections will briefly analyze potential future work for each of these topics.

4.2.1 Dependent Effort Functions $E_i(t)$

If the two patches are harvested by the same harvester, then the effort function is greatly affected. Instead of each $E_i(t)$ being independent, they are interrelated, for example of the manner

$$0 \leq E_1 + E_2 \leq E_{max}. \tag{4.5}$$

This bound is realistic because the combined effort of the two patches cannot exceed the total effort available to the harvester. For example, consider if your harvesting company has 100 boats available to harvest. If there is only one patch to be harvested, all boats can be devoted to that one patch. But if there are multiple patches, those 100 boats must be spread out among all the patches. Thus the effort devoted to harvesting each patch is related to the effort devoted to other patches.

This interdependence of the E_i functions presents an issue. The solution of our ideal E^* is no longer a simple re-arrangement of an equation. Now we must take into account each possible relationship the two effort functions could have to each other.

Consequently, the effort functions available to each patch would be given by the following:

$$\begin{cases} E_1 = E_{max} - E_2, \\ E_2 = E_{max} - E_1. \end{cases} \tag{4.6}$$

So, we have three possibilities for each λ_1 and λ_2:

$$\begin{cases} \lambda_i(0) > p, \\ \lambda_i(0) = p, \\ \lambda_i(0) < p. \end{cases}$$

The accompanying Heaviside effort Function is:

$$E_i(t) = \begin{cases} E_{max}, & \lambda_i(t) < p, \\ E^* = \frac{f(N_{MSY})}{qN_{MSY}}, & \lambda_i(t) = p, \\ 0, & \lambda_i(t) > p. \end{cases} \tag{4.7}$$

In this case, the manner in which the harvester reacts to initial conditions $N_{i0} > N_i^*$ is not so straightforward as in the one patch case. The harvester must understand the relationship between E_1 and E_2 in order to know how to reduce the populations to N_1^* and N_2^* as quickly as possible. There are many possibilities for how the harvester could do this: for example, he could harvest them both with equal intensity ($E_1 = E_2 = \frac{1}{2}E_{max}$) or harvest E_1 twice as intensely as E_2 ($E_1 = 2E_2 = \frac{2}{3}E_{max}$).

The next step is to write the Hamiltonian in terms of either E_1 or E_2 alone by making the substitution

$$E_2 = E_{max} - E_1. \tag{4.8}$$

We then substitute equation (4.8) into the Hamiltonian (2.56) to obtain a new Hamiltonian:

$$H = p_1 q_1 E_1 N_1 + p q_2 N_2 (E_{max} - E_1) + \lambda_1 (f(N_1) - q_1 E_1 N_1) + \lambda_2 (f(N_2) - q_2 N_2 (E_{max} - E_1)), \tag{4.9}$$

which simplifies to:

$$H = E_1 \left[(p_1 - \lambda_1) q_1 N_1 - (p - \lambda_2) q_2 N_2 \right] + E_{max} q_2 N_2 (p - \lambda_2) + \lambda_1 f(N_1) + \lambda_2 f(N_2). \tag{4.10}$$

We know that both E_1 and E_2 are independently constrained by E_{max}. Therefore, upon our substitution of $E_2 = E_1 - E_{max}$ we implement a Bang-Bang Control.

For this equation, we have several possibilities for λ_i:

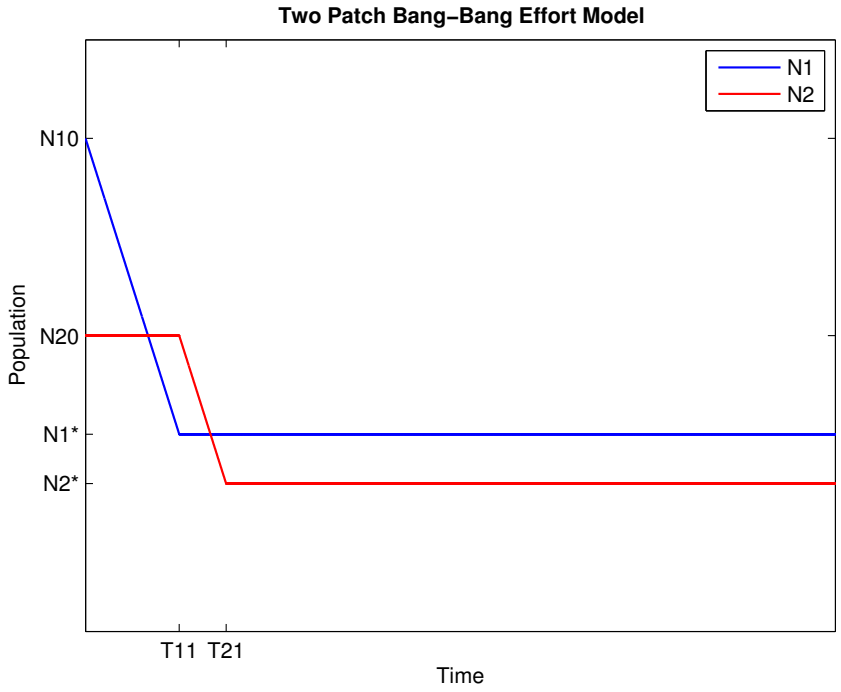

Figure 4.1: $E(t)$ while using Bang-Bang Control to optimize the two-patch model.

$$\begin{cases} \lambda_1 > p, \lambda_2 < p; & E_1 = 0, E_2 = E_{max}, \\ \lambda_1 > p, \lambda_2 > p; & E_1 = 0, E_2 = 0, \\ \lambda_1 < p, \lambda_2 > p; & E_1 = E_{max}, E_2 = 0, \\ \lambda_1 < p, \lambda_2 < p; & E_1 + E_2 = E_{max}. \end{cases} \tag{4.11}$$

We can exclude the second case, as it does not provide any possibility of improving our model, since neither $E_1 = 0$ nor $E_2 = 0$ represent positive harvesting.

Figure 4.1 shows the respective functions of the population N_1 and N_2 as E_1 and E_2 vary over time. This example uses the Bang-Bang Control model: first $E_1 = E_{max}$ and $E_2 = 0$; upon E_1 reaching E_1^*, then $E_1 = 0$ and $E_2 = E_{max}$ until $E_2 = E_2^*$.

Further analysis is required to determine if the Bang-Bang Control is the optimal

method for harvesting two oyster patches - the values of many parameters must be taken into account. For example, the above situation could be reversed: $E_2 = E_{max}$ and then $E_1 = E_{max}$. Or, $E_1 = E_2 = \frac{1}{2}E_{max}$, or $E_1 = \frac{1}{3}E_{max}$ and $E_2 = \frac{2}{3}E_{max}$, or any other combination.

4.2.2 Dispersion Between Two Patches

Dispersion between two patches would make the model more applicable to real-life scenarios. If there exist two oyster patches, Patch A upstream from Patch B, then the flow of the larvae from Patch A downstream to Patch B would be modeled by a dispersion term. Upon reaching Patch B, some larvae would presumably find an appropriate site to settle as spat, adding to the height and health of Patch B.

Dispersion is particularly applicable in the oyster repopulation efforts occurring in the Chesapeake Bay Basin at the moment. Modeling the effectiveness of different types of patch placement could lead to new successes for these repopulation efforts and increase the health of the *Crassostrea virginica* in the Chesapeake Bay Basin. The equations for this sort of model would take the following form:

$$\begin{cases} \dfrac{dN_1}{dt} = f(N_1) - qE_1N_1 - d(N_1 - N_2), \\ \dfrac{dN_2}{dt} = f(N_2) - qE_2N_2 - d(N_2 - N_1), \end{cases} \tag{4.12}$$

where $d(N_i - N_j)$ is the dispersion term mentioned above. If Patch A is upstream from Patch B, it would be logical that $d(N_A - N_B) < 0$ and $d(N_B - N_A) > 0$. However, the addition of this term would also significantly complicate the analytical calculations from the previous chapters.

4.3 Conclusions

Our model has solved for analytical and numerical solutions of optimal control of oyster harvesting for populations demonstrating the Allee Effect. We have solved for equations to determine the optimal sustainable population (N^*) and effort (E^*) for a bang-bang control model. The analytical model also solves for times T_1 and T_2 at which the piecewise Heaviside effort function is switched to E^* and from E^* to E_{max}, respectively. The method of solving for T_1 depends on the initial value of $N_0 = N(0)$.

We have laid the groundwork for extrapolation upon our model. Future work could incorporate inclusion of co-dependence of multiple patches or terms for economic profit and operational cost. This co-dependence could take the form of dependent effort functions $E_i(t)$ or addition of a term allowing for dispersion between multiple patches.

There is much room for expansion upon current scholarship regarding applications of optimal control theory. Much of this possibility stems from the complexity of the interrelated variables affecting marine life, so models will be inherently limited by the amount of variables they can include; the most realistic models would optimize several variables instead of the one we focused on. Only by incorporating several variables can one succeed in using mathematics to develop a successful harvesting strategy.

4.4 Acknowledgements

This research was supported by the College of William & Mary and the National Science Foundation Computational Science training for Undergraduates in the Mathematical Sciences grant NSF DMS-0703532. Thank you to my advisor Professor Junping Shi for his constant guidance and encouragements, and Professor Michael Lewis for his help with my programs.

Chapter 5

Appendices

5.1 One-Patch Program

Below is the program used to graph the analytical solutions to the one patch system.

```
function one_patch12


%%%%%%%%%%%%%%%
% X2 = LAMBDA %
%%%%%%%%%%%%%%%


%declaration of global variables and parameters
global r; global K; global K0; global q; global p;
global N1; global E1; global Emax; global T;
global tev1; global tev2


%assigning parameters
T=3;
tspan=[0 T];
```

```
Emax=5;
r=1; K=20; K0=5; q=1; p=0.5;
N1=(K+K0+sqrt(K^2-K*K0+K0^2))/3;
E1=(r*N1*(N1/K0-1)*(1-N1/K))/(q*N1);

%initial conditions
x0=[10,0.758];
xone=[N1,p];
xthree = x0;

%the events
options1 = odeset('events',@events1);
options2 = odeset('events',@events2);

%solving the equations
[t1,x1,tev1, xev1, ie]=ode45(@f1,tspan,x0,options1);
[t2,x2,tev2, xev2, ie]=ode45(@f2,tspan,xone,options2);

tev1
xev1

tev2
xev2

tspan2=[0 T];
[t3,x3]=ode45(@f3,tspan2,xthree);
```

```
t=0:0.000001:T;
if T > tev1+tev2
        if x0(1) < N1
            Eff=0;
        elseif x0(1) >= N1
            Eff=Emax;
        end
        Efn = Eff+heaviside(t-tev1)*(-Eff+E1)+...
            heaviside(t-(T-tev2))*(Emax-E1);
elseif T<=tev1+tev2
        if T<tev2
            Efn=Emax;
        elseif tev2<T<tev1+tev2
            if x0(1)>N1
                Efn=Emax;
            elseif x0(1)<N1
                disp(N1)
                Efn=0+heaviside(t-(T-tev2))*Emax;
            end
        end
end

mean(q*Efn*x3(1))

t4=[tev1 T-tev2];
vecN1=zeros(size(t4)); vecN1=vecN1+N1;
vecp=zeros(size(t4)); vecp=vecp+p;
```

```
%%%%%%%%%%%%%    GRAPHS     %%%%%%%%%%%%%%%%%%%%%%

%graph of all effort together
subplot(3,1,1)
plot(t,Efn,'linewidth',1);
axis([0 T -0.1 Emax+0.5])
set(gca,'XTick',[tev1 T-tev2])
set(gca,'YTick',[0 E1 Emax])
set(gca,'XTickLabel','t1|t2')
set(gca,'YTickLabel','0|E*|Emax')
xlabel('time');
ylabel('total effort');

%graph of population total
subplot(3,1,2)
plot(t1,x1(:,1),'linewidth',1);
hold on
plot(t4,vecN1,'linewidth',1);
plot(t2+(T-tev2),x2(:,1),'linewidth',1);
axis([0 T -0.1 N1+2])
set(gca,'XTick',[tev1 T-tev2])
set(gca,'YTick',[0 N1])
set(gca,'XTickLabel','t1|t2')
set(gca,'YTickLabel','0|N*')
xlabel('time');
ylabel('total population');
```

```
%graph of lambda in total
subplot(3,1,3)
plot(t1,x1(:,2),'linewidth',1);
hold on
plot(t4,vecp,'linewidth',1);
plot(t2+(T-tev2),x2(:,2),'linewidth',1);
axis([0 T 0 1]);
set(gca,'XTick',[tev1 T-tev2])
set(gca,'YTick',[0 p])
set(gca,'XTickLabel','t1|t2')
set(gca,'YTickLabel','0|p')
xlabel('time');
ylabel('total lambda');

%%%%%%%%%%%%%%%%%%%%%%%%%%%%%%%%%%%%%%%%%%%%%%%%%%%%

function dxdt=f1(t,x)
    if x0(1) < N1
        E=0;
    elseif x0(1) > N1
        E=Emax;
    elseif x0(1) == N1
        E=Emax;
    end
dxdt=[r*x(1)*(x(1)/K0-1)*(1-x(1)/K)-q*E*x(1);
    -q*(p-x(2))*E-x(2)*(r/(K0*K))*(-3*(x(1))^2+2*(K0+K)*x(1)-K0*K)];
```

```
end

function dxdt=f2(t,x)
dxdt=[r*x(1)*(x(1)/K0-1)*(1-x(1)/K)-q*Emax*x(1);
    -q*(p-x(2))*Emax-x(2)*(r/(K0*K))*(-3*(x(1))^2+2*(K0+K)*x(1)-K0*K)];
end

function dxdt=f3(t,x)
    if T > tev1+tev2
        if x0(1) <= N1
            Eff=0;
        elseif x0(1) > N1
            Eff=Emax;
        end
        Efn = Eff+heaviside(t-tev1)*(-Eff+E1)+...
            heaviside(t-(T-tev2))*(Emax-E1);
    elseif T<=tev1+tev2
        Efn = Emax;
    end
dxdt=[r*x(1)*(x(1)/K0-1)*(1-x(1)/K)-q*Efn*x(1);
    -q*(p-x(2))*Efn-x(2)*(r/(K0*K))*(-3*(x(1))^2+2*(K0+K)*x(1)-K0*K)];
end

function [value,isterminal,direction] = events1(t,x)
    value =x(1)-N1;
    isterminal=1;
    direction=0;
```

```
end

function [value,isterminal,direction] = events2(t,x)
    value =x(2);
    isterminal=1;
    direction=0;
end

end
```

5.2 Forward-Backward Sweeping Code

Below is the code for our fourth-order Runge-Kutta simulation.

```
function y = attempt8_code(k0,k,r,q,p,N0,Emax,T)

test = -1;
global delta r p q k0 k N0 N h h2 N1 E1
delta = 0.001;
N = 10;
t = linspace(0,T,N+1);
h = T/N;
h2 = h/2;

u = zeros(1,N+1);
x = zeros(1,N+1);
lambda = zeros(1,N+1);
```

```
lambda(N+1)=0;

x(1) = N0;

N1=(k0+k+sqrt(k^2-k0*k+k0^2))/3;
E1=(r*N1*(N1/k0-1)*(1-N1/k))/(q*N1);
counter = 0;

while(test < 0)
    disp('in while');
    counter = counter + 1
    oldu = u;
    oldx = x;
    oldlambda = lambda;

    for i = 1:N
        k1 = h*f(t(i),u(i),x(i));
        k2 = h*f(t(i) + h/2, 0.5*(u(i) + u(i+1)), x(i) + k1/2);
        k3 = h*f(t(i) + h/2, 0.5*(u(i) + u(i+1)), x(i) + k2/2);
        k4 = h*f(t(i + 1), u(i + 1), x(i) + k3);
        x(i+1) = x(i) + (1/6)*(k1 + 2*k2 + 2*k3 + k4);
    end

    for i = 1:N
        j = N + 2 - i;
        k1 = h*g(u(j), lambda(j), x(j));
        k2 = h*g(0.5*(u(j) + u(j-1)), lambda(j) - k1/2, ...
```

```
        0.5*(x(j) + x(j-1)));
    k3 = h*g(0.5*(u(j) + u(j-1)), lambda(j) - k2/2, ...
        0.5*(x(j) + x(j-1)));
    k4 = h*g(u(j - 1), lambda(j) - k3, x(j-1));
    lambda(j-1) = lambda(j) - (1/6)*(k1 + 2*k2 + 2*k3 + k4);
end

u1 = zeros(1,N+1);
for i=1:N+1
    %temp is partial Hamiltonian partial Effort
    temp = q*(p-lambda(i))*x(i);
    if(temp>1.0e-8);
        u1(i) = Emax;
    elseif(temp<-1.0e-8);
        u1(i) = 0;
    else
        disp('NOPE')
        disp(temp)
        disp(x(i));
        disp(lambda(i));
        u1(i) = E1;
    disp(lambda)
    end
end

w=0.5;
u = w*u1 + (1-w)*oldu;
```

```
    temp1 = delta*sum(abs(u)) - sum(abs(oldu - u));
    temp2 = delta*sum(abs(x)) - sum(abs(oldx - x));
    temp3 = delta*sum(abs(lambda)) - sum(abs(oldlambda - lambda));
    disp(temp1);
    disp(temp2);
    disp(temp3);
    test = min(temp1, min(temp2, temp3))
end
disp('out of while');

y(1,:) = t;
y(2,:) = x;
y(3,:) = u;
y(4,:) = lambda;
end

function forward=f(t,u,x)
global delta r p q k0 k N0 N h h2 N1 E1
forward = r*x*(x/k0-1)*(1-x/k)-q*u*x;
end

function backward=g(u,lambda,x)
global delta r p q k0 k N0 N h h2 N1 E1
backward = -q*(p-lambda)*u-(lambda*r/(k*k0))*(-3*x^2+2*x*(k+k0)-k*k0);
end
```

Bibliography

[1] Alford, John J. The Chesapeake Oyster Fishery. Annals of the Association of American Geographers, Vol. 65 No. 2 (Jun. 1975), pp. 229-239.

[2] Allee, W.C., Emerson, A.E., Park, O., Park, T. and Schmidt, K.P. (1949). Principles of animal ecology. Saunders Co., Philadelphia, 1949.

[3] Arrow, Kenneth J.; Bensoussan, Alain; Feng, Qi; Sethi, Suresh P. Optimal Savings and the Value of Population. Proceedings of the National Academy of Sciences of the United States of America, Vol. 104, No. 47 (Nov. 20 2007), pp. 18421-18426.

[4] Bailey, K. Holder; Polis, G. A. Optimal and Central-Place Foraging Theory Applied to a Desert Harvester Ant. Oecologia, Vol. 72, No. 3 (1987), pp. 440-448. Springer in cooperation with International Association for Ecology, 1987.

[5] Clark, Colin W. Mathematical bioeconomics. The mathematics of conservation. Third edition. Pure and Applied Mathematics (Hoboken). John Wiley & Sons, Inc., Hoboken, NJ, 2010.

[6] Dennis, Brian. Allee Effects in Stochastic Populations. Oikos, Vol. 96, No. 3 (Mar., 2002), pp. 389-401. Blackwell Publishing on behalf of Nordic Society Oikos, 2002.

[7] Flores, José D. Harvesting Single Population. Department of Mathematical Sciences, University of South Dakota. April 2011.

[8] Jordan-Cooley, William C.; Lipcius, Romauld N.; Shaw, Leah B.; Shen, Jian; Shi, Junping. Bistability in a differential equation model of oyster reef height and sediment accumulation. Journal of Theoretical Biology 289, 1-11. Elsevier, 2011.

[9] Kot, Mark. Elements of mathematical ecology. Cambridge University Press, Cambridge, 2001.

[10] Lenhart, Suzanne; Workman, John T. Optimal control applied to biological models. Chapman & Hall/CRC Mathematical and Computational Biology Series. Chapman & Hall/CRC, Boca Raton, FL, 2007.

[11] Lenihan, Hunter S.; Peterson, Charles H.; Byers, James E.; Grabowski, Jonathan H.; Thayer, Gordon W.; Colby, David R. Cascading of Habitat Degradation: Oyster Reefs Invaded by Refugee Fish Escaping Stress. Ecological Applications, Vol. 11 No. 3 (Jun. 2001), pp. 764-782. Ecological Society of America, 2001.

[12] Richardson, James W.; Ray, Daryll E. Commodity Programs and Control Theory. American Journal of Agricultural Economics, Vol. 64, No. 1 (Feb. 1982), pp. 28-38. Oxford University Press on behalf of the Agricultural & Applied Economics Association, 1982.

[13] Sharp, J.A. Capital Investment – An Optimal Control Perspective. The Journal of the Operational Research Society, Vol. 41, No. 11 (Nov. 1990), pp. 1053-1063. Palgrave Macmillan Journals on behalf of the Operational Research Society, 1990.

[14] Sherk Jr., J. Albert. Current Status of the Knowledge of Biological Effects of Suspended and Deposited Sediments in the Chesapeake Bay. Chesapeake Science, Vol. 13, Supplement: Biota of the Chesapeake Bay (Dec. 1972), pp. S137-S144. Coastal and Estuarine Research Foundation, 1972.

[15] Shi, Junping; Shivaji, Ratnasingham. Persistence in reaction diffusion models with weak Allee effect. Journal of Mathematical Biology. Springer-Verlag, 2006.

[16] Stephens, P.A.; Sutherland, W.J.; Freckleton, R.P. What is the Allee Effect? Oikos, Vol. 87, No. 1 (Oct., 1999), pp. 185-190. Blackwell Publishing on behalf of Nordic Society Oikos, 1999.

[17] Vincent, Thomas L. Pest Management Programs via Optimal Control Theory. Biometrics, Vol. 31, No. 1 (Mar., 1975), pp. 1-10. International Biometric Society, 1975.

[18] Wang Jing; Wang, Ke. Optimal control of harvesting for single population. Appl. Math. Comput. 156 (2004), no. 1, 235–247.

[19] Wang, Jing; Wang, Ke. Optimal harvesting policy for single population with stage structure. Comput. Math. Appl. 48 (2004), no. 5-6, 943–950.